

## Vortex motion of laser plasma

© A.A. Voskoboev, V.S. Mezhevov, M.D. Taran, S.P. Yatskov

Troitsk Institute for Innovation and Fusion Research, Russian Academy of Sciences, Troitsk, Moscow, Russia  
 e-mail: voskoboev.a@triniti.ru, mezhevov@triniti.ru

Received November 21, 2023 Revised April 19, 2024 Accepted April 25, 2024

The observation of toroidal plasma vortices formed when the radiation of a repetitively pulsed CO<sub>2</sub> laser was applied to a pyrographite target in a helium atmosphere are reported. The results of numerical calculations of the experimental model corresponding to the experiment are presented. The lifetime of the toroidal rings is shown to be more than 100 μs.

**Keywords:** Plasma vortices, Plasma spectroscopy, repetition rate pulsed CO<sub>2</sub> laser.

DOI: 10.61011/TP.2024.06.58821.290-23

### Introduction

Many studies are dedicated to research of plasma vortices formed from plasma leakage in impulse plasmatrons [1–7]. Special attention is paid to toroidal vortex formations having high stability, duration of existence and directionality of movement. There is an assumption [1] that such plasma motion may contribute to ball lightning generation.

To study vortex movement of plasma in gas medium, plasmatrons of low volume with cylindrical shape are used [5,6], which are separated from the output side by a thin partition destroyed by developed high pressure. Plasma is generated by electric discharge in gas filling the plasmatron with duration of 10<sup>-4</sup>–10<sup>-3</sup> s and specific energy contribution from 0.01 to 3 kJ/cm<sup>3</sup>. After the discharge, the plasma leaks into air or into gas-filled volume, besides, plasma leakage from the discharge chamber is accompanied by formation of plasma vortices.

During our studies of diamond-like coating sputtering using a pulse-periodic CO<sub>2</sub>-laser as shown in paper [8], generation of a plasma „jet“ was discovered. To explain this effect, some measurements and numerical calculations were carried out, which demonstrated the possibility of large-scale plasma vortices occurrence under exposure to impulse laser.

### 1. Experimental setup description

In the experiments [8] a pulse-periodic CO<sub>2</sub>-laser was used with a closed gas circuit and pulse repetition rate of up to 200 Hz. An emission impulse with energy of 1.2 J consisted of a peak with duration of around 0.3 μs at the base and a falling tail with duration of 3 μs. The peak power of laser emission was around 1.5 MW. Temporal shape of the emission pulse is shown in Fig. 1.

Emission of the pulse-periodic CO<sub>2</sub>-laser was fixed with a lens from KCl with a focal distance of 26 cm on a target installed in a cylindrical chamber with length of 15 cm and diameter of 13 cm via a window from KCl. The diameter of the focused emission on the target surface is around 0.6 mm.

Density of laser emission power in the lens focus was 6 · 10<sup>8</sup> W/cm<sup>2</sup>.

Photography, temporal and spectral diagnostics of plasma emission were carried out via the side windows of the chamber. The plasma image was projected with the help of a lens at the end of the optical fiber with diameter of 200 μm installed in the image plane. The fiber end could move in the image plane. Optical fiber was connected to a photodetector of PDA36A-EC type by THORLABS, connected to an oscilloscope. The chamber was pumped with an oil-free pump to pressure of 50 Pa.

Experiments on interaction were carried out using a pyrographite target with thickness of 4 mm. Fig. 2 shows the diagram of target installation.

The target is fixed on the support, which could move along the beam axis. A tube of several layers of nickel foil was also installed on the same support and pressed tightly with its end to the target surface. The tube was installed

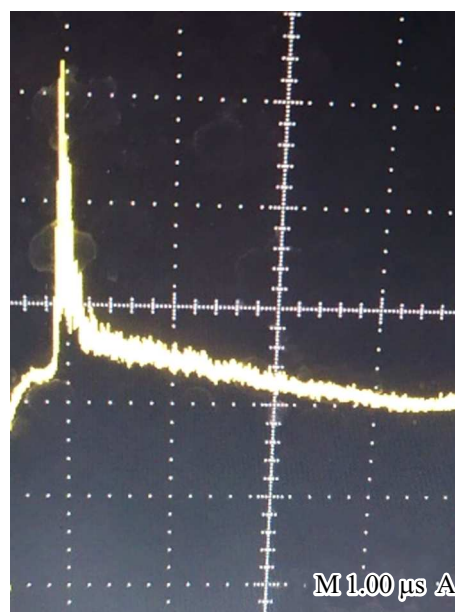
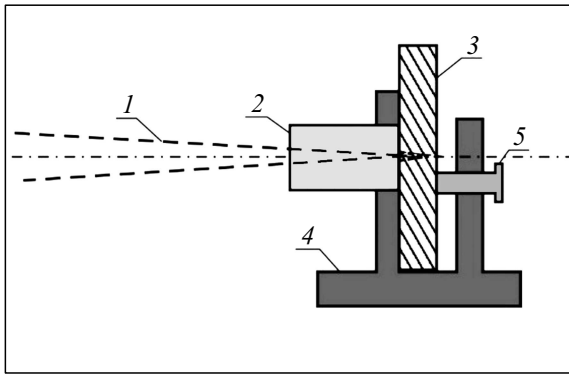
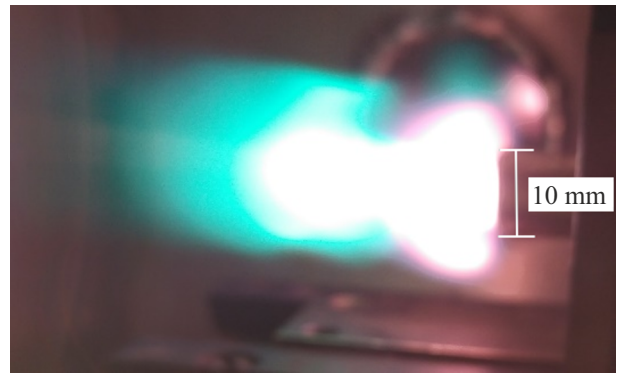


Figure 1. Emission pulse shape.



**Figure 2.** Target fixation diagram: 1 — laser beam, 2 — tube, 3 — target, 4 — support, 5 — target fixation system.



**Figure 3.** Time-integral photograph of plasma (one impulse) in the beginning of radiation process, at delay time of 1 s.

for the ability to create a directed motion of carbon plasma towards the sputtered sample. Tube length — 16 mm, inner diameter — 10 mm, wall thickness — 0.2 mm.

## 2. Experimental results

The interaction chamber was vacuumized and filled with helium to the pressure of 4000 Pa. At pulse repetition rate of more than 10 Hz a plasma flux was observed at the initial period (Fig. 3).

After the pulse repetition rate increased to 10–50 Hz in 1–2 min of interaction the type of plasma changes significantly (Fig. 4, *a*).

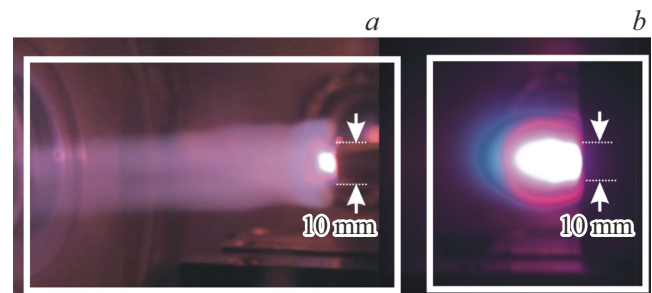
Intensity of plasma glow on the tube cut during the long-term operation drops significantly, a „jet“ appears, which is observed visually only in pulse-periodic mode (more than 10 Hz) due to low intensity of plasma flux glow. Vortex motion is indicated by the shape of plasma formation on the tube cut and rectilinear motion without transverse expansion by more than 10 calibers of the tube. The transverse dimension of the vortex formation is twice more than the inner diameter of the tube. Laser beam diameter at the tube inlet is around 2 mm.

Using Thorlabs CCS100 spectrometer, spectra were read, and plasma qualitative composition was assessed. Fig. 5 shows the spectrum obtained in the beginning of target radiation, with a spectrometer focus tuned to the middle of the plasma formation at the distance of 10 mm from the tube. The spectrum is qualitatively specific both for Fig. 3 and for 4, *b*.

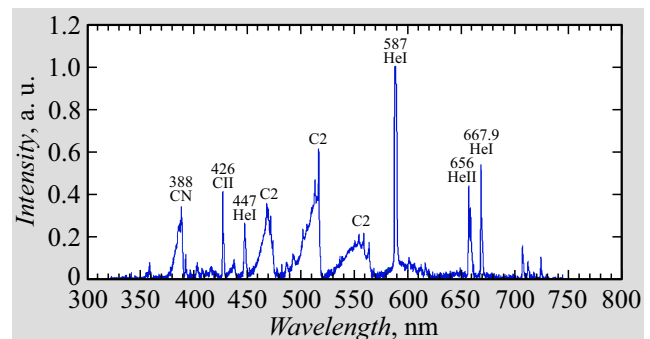
Green-blue color is explained by Swan bands for carbon radicals  $C_2$  in the area of 460 and 520 nm, which are formed in process of carbon plasma cooling. Red color is provided for by He lines at 587, 656 and 667.9 nm.

Fig. 6 shows the spectrum specific for plasma formations shown in Fig. 4, *a*, obtained in the center of plasma formation at the distance of 20 mm from the tube.

A CN — 388 nm band and three intense helium lines HeI — 587, 667.9 and HeII — 656 nm are seen. Swan bands are hardly visible.



**Figure 4.** Photographs of plasma formations, exposure 1 s, at repetition rate of 10 Hz: *a* — with a tube, *b* — with a hole in graphite.



**Figure 5.** Spectrum of emission of plasma formations at initial impulses.

Distribution of intensity in the image of the plasma flux (lower intensity in the central part) and rectilinearity of the motion at the large distance from the tube cut indicate, in our opinion, the toroidal vortex motion of plasma. Weak intensity of toroidal vortex glow prevents high speed shooting, therefore, a photodetector with optic fiber input was used to research temporal characteristics of the plasma flux. Oscillograms of plasma glow from one impulse on the axis of the plasma flux on the tube cut (*a*) and at the distance of 4 cm from the cut (*b*) are shown in Fig. 7.

The first peak in Fig. 7, *b* depends on reflection of plasma flow from the tube on the inner surfaces of the chamber,

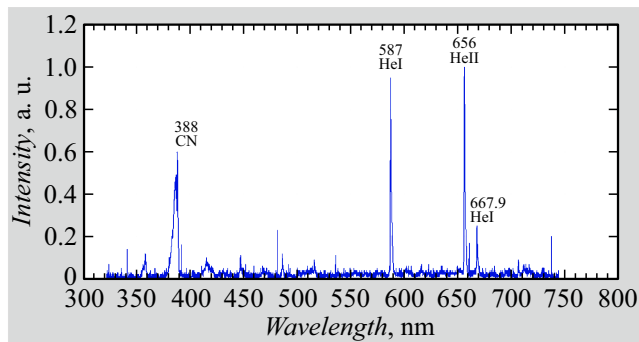


**Figure 6.** Spectrum of emission of plasma formations under long-term radiation in „jet“.

besides, the sensitivity of the photodetector is significantly increased by adjustment of the gain factor of a preliminary amplifier.

Average speed of vortex motion along the tube axis defined by time delay is around 450 m/s. Plasma glow on the tube cut starts in 4  $\mu$ s after the start of target surface exposure to laser emission.

Change of the mode of interaction with the target seems to be related to formation of a cone cavity in a graphite target with an inlet diameter of 0.8 mm and depth of 3 mm, which reduces laser emission energy density on the surface of the carbon target and accordingly the density of carbon vapors. In this case the low concentration of carbon vapors provides for laser-induced breakdown and absorption of laser emission in helium, at the same time mostly helium plasma is formed (which is confirmed by registration of the plasma vortex spectrum registration). Further gas dynamic process of plasma formation expansion and tube pressure balancing happens, which is followed by the plasma leakage process.

To confirm this assumption, a plasma formation was photographed near the target without a shaping tube after cone hole formation. The photograph of plasma formation (from one impulse) is shown in Fig. 8. To observe the structure of plasma formation, a neutral filter with triple weakening was applied. The photo shows the zone of maximum plasma heating, with diameter of around 3 mm and length of around 10 mm, which considerably differs from the structure of plasma formation in vacuum under the same conditions [8].

Temperature was assessed by measurements of the spectrum in paper [8], where temperature was detected at the distance of 18 mm from the target and made around 6000 K.

It should be noted that formation of plasma vortices was affected by the shape of the outlet hole of the tube. Experiments were carried out with a hole in a massive graphite with parameters similar to the tube dimensions (diameter 10 mm, depth 16 mm). In such a configuration no long-lived plasma formations were observed. A photograph of plasma formations in this case is shown in Fig. 4, *b*. In our

experiments, obviously, a thin-walled outlet end of the tube facilitates occurrence of toroidal vortices.

When a copper plate was used as a target, vortex toroidal motion of plasma was also observed, but intensity of plasma formation flow was significantly weaker.

Vortex motion was observed in the helium pressure range from 10 to 100 (1330–13000) Torr (Pa).

### 3. Numerical experiments

To estimate parameters of the flow occurring near the tube, with the geometric dimensions of the tube used in the experiment, at a single impulse of laser emission, numerical experiments were carried out using package ANSYS 2021R2 [9], of Fluid Flow (Fluent) software (license: Customer # 1084164).

For numerical modeling of the live experiment a closed axisymmetric estimated area was selected. A metal cylindrical tube with wall thickness of 1 mm and inner radius of 5 mm is attached to the left boundary of the estimated area so that the axis of the tube matches the axis  $z$  of the estimated area, tube length is 16 mm. Example of estimated area along axis  $z$  —  $L_z = 56$  mm, radius of estimated area  $r = 65$  mm. To describe medium flow, a model of an ideal gas (helium) was selected, full Navier–Stokes equations were solved in axisymmetric geometry with account of heat conductivity with the assumption of the laminar viscosity model. Note that in this variant (and we confirmed it numerically) it was sufficient to use Euler equations for adequate description of the vortex motion, which do not take into account the heat conductivity and viscosity effects, since for the time of calculation these effects „fail“ to impact the nature of the flow, and the vortex is formed by a heterogeneous pressure field. No plasma effects were taken into account in the model. Besides, the presence of carbon admixtures in gas was not taken into account as well, all effects with energy absorption on this admixture manifested themselves in temperature field at the initial moment of time. At the rigid boundaries of the area, zero speed conditions were set, and a laminar viscosity model was selected.

Background pressure of helium in the chamber is  $P_0 \approx 0.04$  atm  $\approx 30$  Torr  $\approx 4000$  Pa.

At the initial moment of time on the constant density background a temperature disturbance is created near the axis and the origin of coordinates, which complies with the distribution of maximum intensity of the flow shown in figure 8, in the form of

$$T_0[\text{K}] = 300 + 10^4 \cdot \exp(-r^2/4 \cdot 10^{-6} - z^2/1.96 \cdot 10^{-4}).$$

Here temperature is in K, and distance is in m.

For the estimate it was assumed that all energy of the laser impulse is absorbed in helium in the central part of the tube according to Fig. 8. The estimated pressure maximum

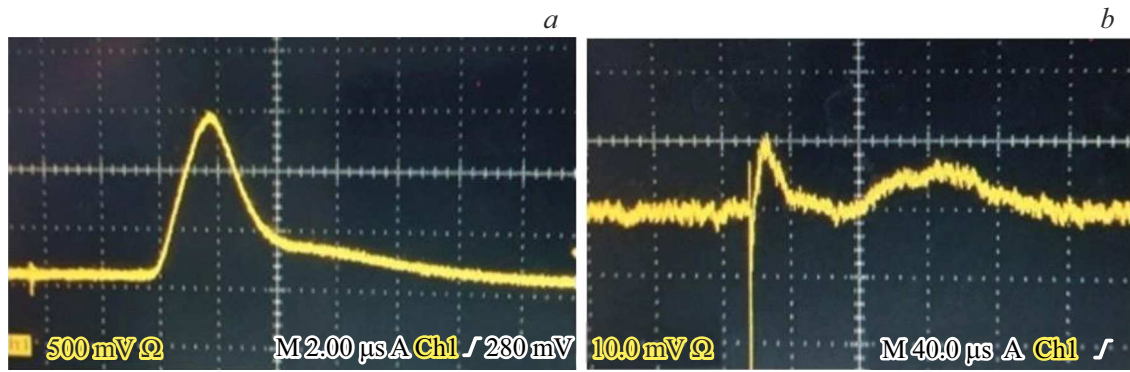


Figure 7. Oscillogrms of plasma glow on tube cut (a) and 4 cm away from the cut (b).

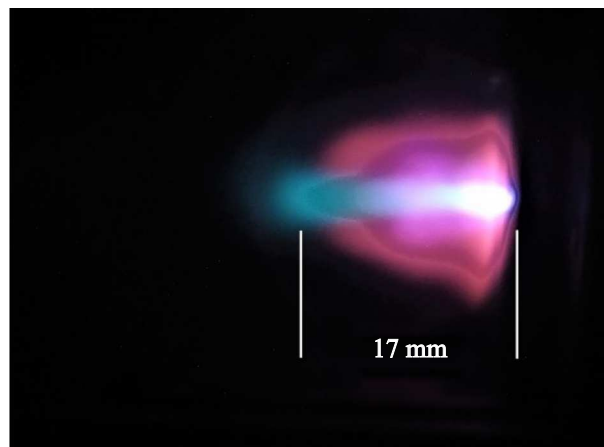


Figure 8. Time-integral photo of plasma in absence of tube upon cone crater formation.

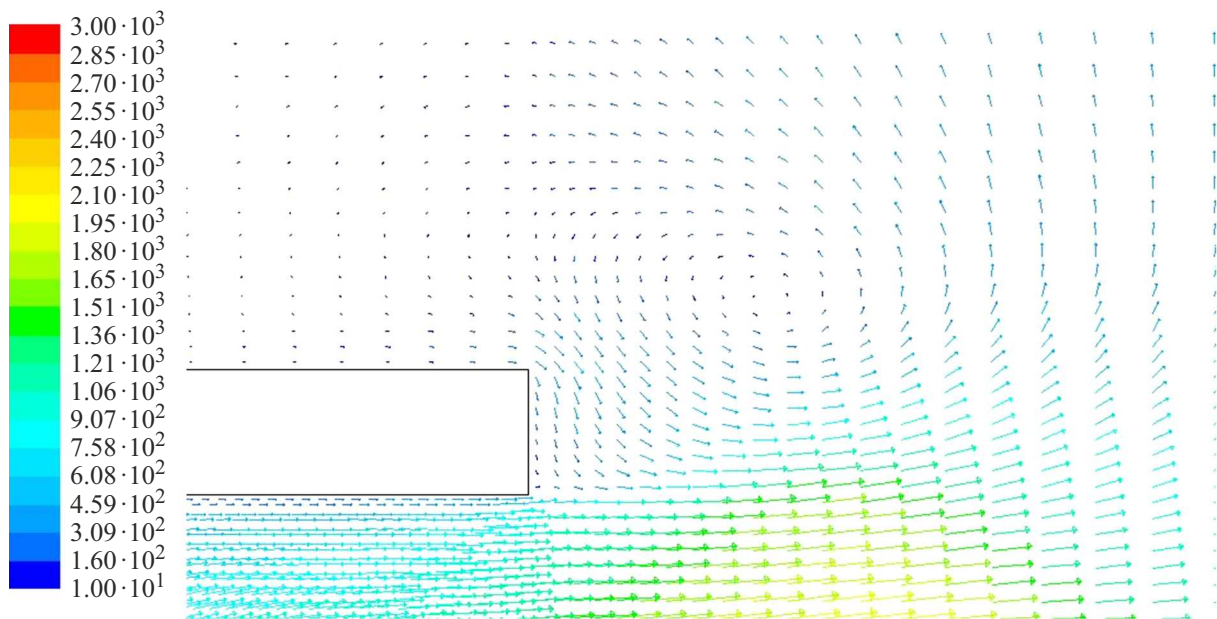
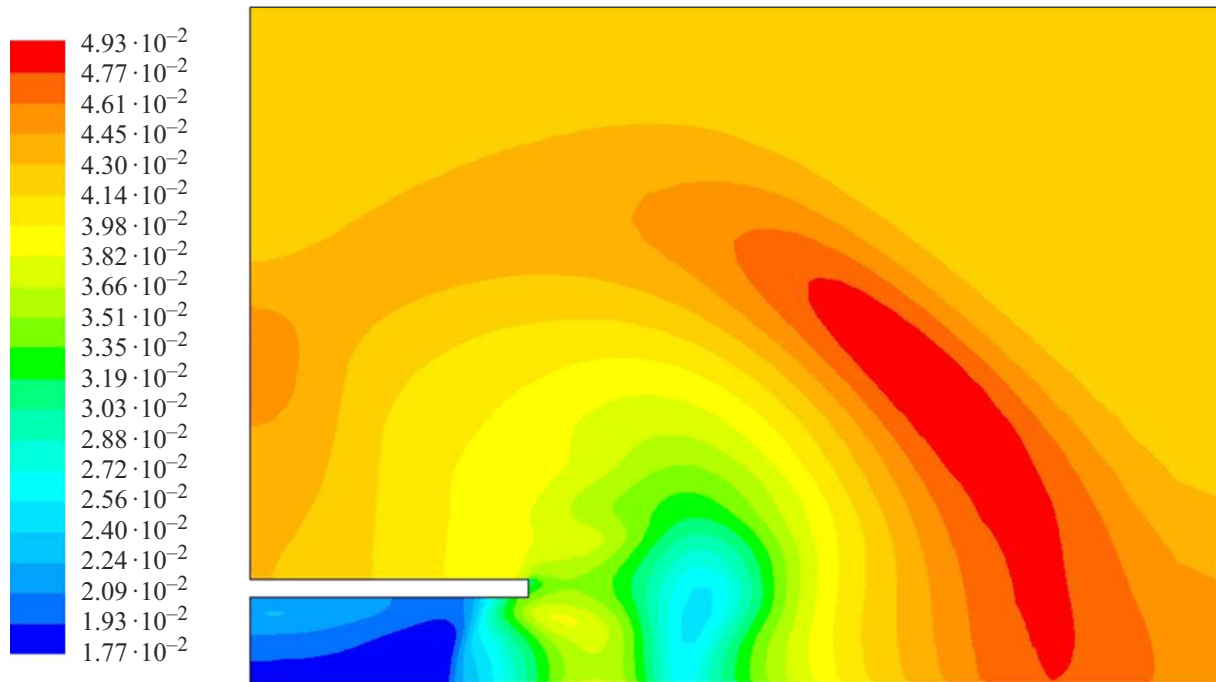
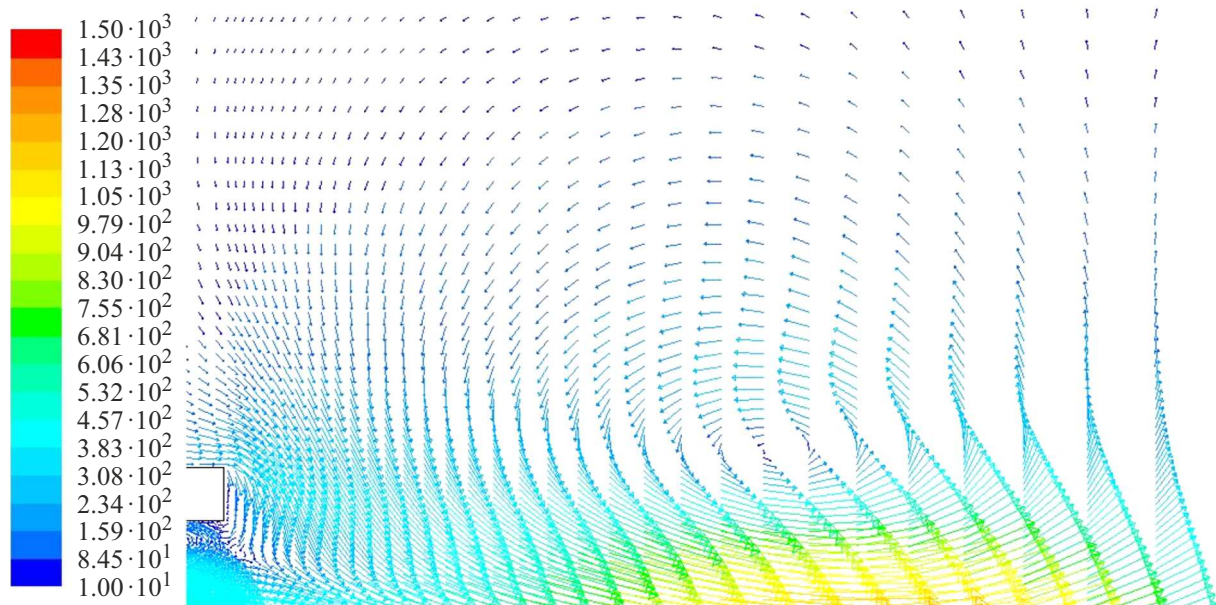


Figure 9. Distribution of speed vector in estimated area at moment of time  $t \approx 10.4 \mu s$ .



**Figure 10.** Distribution of pressure in estimated area at moment of time  $t \approx 24.0 \mu\text{s}$ .



**Figure 11.** Distribution of speed vector in estimated area at moment of time  $t \approx 24.0 \mu\text{s}$ .

is in the origin of coordinates and is  $P_{\max} \approx 1.42 \text{ atm}$ , and the estimated maximum of temperature is  $T_{\max} = 10\,300 \text{ K}$ .

Fig. 9 shows the field of speed vector in the estimated area at the moment of time  $t \approx 10.4 \mu\text{s}$ . You can see that the center of the formed vortex is located approximately 2 mm to the upper edge of the shaping tube and approximately 1 mm above its outer surface. Maximum value of speed in the estimated area is  $V_{\max} \approx 3\,000 \text{ m/s}$ . The vortex is formed, obviously, by the formed distribution of pressure.

Fig. 10 shows the pressure field in the estimated area at the moment of time  $t \approx 24.0 \mu\text{s}$ . You can see that maximum pressure dropped and exceeds the background value approximately by 20%, and the minimum value practically did not change, but stays within the ring.

Besides, there is an area of lower pressure (approximately 1.5 times below the background one, in the minimum, to the right from the cut by approximately 10 mm). Fig. 11 shows the field of speed vector in the estimated area at the

same moment of time. You can see that the center of vortex moved substantially to the center of the estimated area and is located at 10 mm from the tube cut and practically at the level of the outer boundary of the ring. Estimate of speed of vortex center movement towards the center of the area is  $V_{\text{vor}} \approx 570$  m/s. Maximum value of the flow speed at this moment of time is  $V_{\text{max}} \approx 1500$  m/s. At this moment of time the specific radial dimension of the vortex is  $L_r \approx 14$  mm, and axial one is  $L_z \approx 20$  mm.

## Conclusion

Under pulse-periodic interaction of laser mission of a CO<sub>2</sub>-laser with a graphite target and a tube installed near the focus that generates a plasma flow, a formation of long-lived plasma vortices was observed.

Duration of plasma vortices existence exceeds 100  $\mu$ s with laser impulse duration of 3  $\mu$ s.

Occurrence of vortices depends on the temporal shape of the laser impulse, composition of the gas medium and status of the target surface.

The numerical experiment in this case shows that a large-scale vortex may be created and may exist for a long period of time. Pressure rise in the high-temperature part of the estimated area vs the background value complies with the experiments with toroidal plasma vortices carried out at atmospheric pressure.

There is no conflict between live and numerical experiments. On the contrary, the numerical experiment clearly shows the vortex motion of the flow observed in the live experiment.

## Conflict of interest.

The authors declare that they have no conflict of interest.

## References

- [1] A.M. Andrianov, V.I. Sinitsyn. ZhTF, **47** (11), 1318 (1977) (in Russian).
- [2] A.F. Aleksandrov, B. Azzeddin, M.G. Skvortsov i dr. *Tez. dokl. IX Vses. konf. po generatoram nizkotemperaturnoy plazmy* (Frunze, Ilim, 1983), p. 402-403 (in Russian).
- [3] A.F. Aleksandrov, Yu. Bakhgat, M.G. Skvortsov, I.V. Timofeev, V.A. Chernikov, U. Yusupaliev. ZhTF, **56** (12), 2392 (1986) (in Russian).
- [4] A.F. Aleksandrov, I.V. Timofeev, V.A. Chernikov, U. Yusupaliev. TVT, **26** (4), 639 (1988) (in Russian).
- [5] U. Yusupaliev. ZhTF, **74** (7), 52 (2004) (in Russian).
- [6] U. Yusupaliev, P.U. Yusupaliev, S.A. Shuteev. ZhTF, **77** (7), 50 (2007) (in Russian).
- [7] M.N. Zharnikov, A.S. Kamrukov, I.V. Kozhevnikov, N.P. Kozlov, I.A. Roslyakov. ZhTF, **78** (5), 38 (2008) (in Russian).
- [8] A.A. Voskoboev, A.N. Kirichenko, V.S. Mezhevov, S.P. Yatskov. ZhTF, **93** (11), 1679 (2023) (in Russian). DOI: 10.61011/JTF.2023.11.56501.196-23

- [9] Electronic source. Available at: URL: <https://www.ansys.com/>

*Translated by M. Verenikina*